Baseline trabecular bone and its relation to incident radiographic knee osteoarthritis and increase in joint space narrowing score: directional fractal signature analysis in the MOST study

APPENDIX

1. Acquisition of radiographs

Knees were flexed at 20-30° and feet were externally rotated 10° using a plexiglass positioning frame (SynaFlexer Synarc^{TM}, San Francisco, California).

The following radiographic systems and resolutions were used:

- UAB (Computer radiography (CR)): A Agfa ADC System, Quantum Q-Rad CR-based imaging system was used with 149 dpi resolution (pixel spacing = 0.17mm). Images of knees were stored in 12 bit DICOM format.
- UIowa (Digitized film (DF)): Radiographs were acquired with a Bucky screen technique and a film/screen speed of 200-400. Film radiographs were digitized using a Lumisys film scanner with a scan mode of 16-bits and optical resolution of 254 dpi (pixel spacing = 0.1mm), then stored as 16-bit DICOM images.

For both UIowa and UAB the imaging voltage was set to 70 kVp and the film-to-focus distance was 72 inches. The exposure was varied from 5 to 12 mA/s and from 7 to 13 mA/s respectively. Both knees were imaged at the same time on imaging plate (UAB) or 14″×17″ film (UIowa).

For measurement of knee alignment, bilateral full-limb radiographs were acquired using the method of Sharma et al. [1].

2. Grading of knee radiographs

An experienced rheumatologist and a musculoskeletal radiologist who were blind to clinical data, graded PA radiographs according to the KL and individual features including JSN and osteophytes. The individual features were graded 0-3 using the Osteoarthritis Research Society International (OARSI) atlas. The readers also graded lateral radiographs using the Framingham Study protocol [2]. Disagreement on incidence and prevalence of OA and JSN progression were adjudicated by three readers. Osteophyte grades were not adjudicated. The weighted kappa coefficients for agreement between the two readers on osteophytes were 0.63 (overall), 0.63 (medial) and 0.62 (lateral) for PA view.

A partial grade for change was used if JSN worsened, but did not achieve a full grade change longitudinally. Disagreements as to whether half-grade or full-grade increase occurred were not adjudicated. The weighted Kappa values for inter-reader agreement on half-grade increase was 0.58 and on either half or full-grade increase was 0.66 [3].

3. Measurement of knee alignment

Knee alignment was assessed using the hip-knee-ankle (HKA) angle measured from baseline full-limb radiographs using the Surveyor 3 image analysis software tool (OAISYS Inc., Kingston, Ontario, Canada). Neutral alignment was defined as HKA between 178^{o} and 182^{o}. Varus malalignment was defined as HKA $<178^{o}$ and valgus malalignment as HKA $>182^{o}$. The inter- and intra-reader intraclass correlation coefficients for HKA angle were 0.95 and 0.96 [4].

4. Accuracy of bone region selection

The similarity index and offsets calculated between the regions (132 knees) selected by the automated method and the "gold standard" regions (radiologist expert) were greater than 0.8 and [-1.78, 1.27]×[0.26, -0.65] mm (medial) and [-2.15, 1.59]×[0.52, -0.58] mm (lateral) respectively [5]. The selection of a single region took ~0.5 min (Matlab running on a Unix computer with a 1.2 GHz clock).

We visually checked regions selected by the automated method, and 451 out of 4104 = 2 × (894 + 1158) (about 11%) regions were manually adjusted. Errors were caused by a low contrast at the tibio-fibular joint, low contrast of borders of the knee joint, or by the overlap of calibration markers of other objects with the edge of the tibia. There were no errors due to structural features typical of OA. This was expected since at baseline, the knees all had KL grade 0 or 1.

5. Fractal analysis

5.1. A description of the variance orientation method

Texture data is a digital image defined as a function $z = \mathrm{I}(x, y)$ which assigns a grey-scale level value $z \in Z$ to a pixel located at $(x, y) \in X \times Y$. Assuming that $z = \mathrm{I}(x, y)$ is generated by a fractal Brownian function, the variance of differences $\mathrm{I}(\mathbf{x} + \Delta\mathbf{x}) - \mathrm{I}(\mathbf{x})$ is related to the distance between a pair of points $||\Delta\mathbf{x}||$ (Fig. 1a) as follows [6,7]:

$$\mathrm{VAR}[|\mathrm{I}(\mathbf{x} + \Delta\mathbf{x}) - \mathrm{I}(\mathbf{x})|] \propto ||\Delta\mathbf{x}||^{2H}$$

where $\mathbf{x} = (x, y)$ is the coordinate vector and H is the Hurst coefficient. By plotting variances against distances (for all $\mathbf{x}$ and $\Delta\mathbf{x}$) in log–log coordinates and fitting a line to the plot, H is calculated as a half of the slope of the line fitted (Fig. 1b) [7].

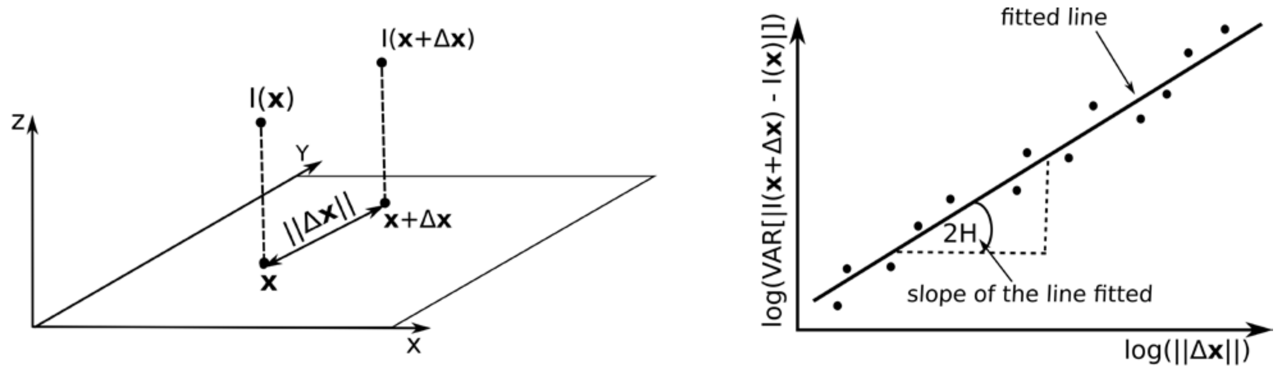

(a) (b)

Fig. 1. Schematic illustration of (a) the difference $\mathrm{I}(\mathbf{x} + \Delta\mathbf{x}) - \mathrm{I}(\mathbf{x})$ and the distance $\|\Delta\mathbf{x}\|$, and (b) the log-log plot of variances against distances with the line fitted and the Hurst coefficient H.

The Hurst coefficients are calculated at different scales and directions. The direction is defined as an angle θ between the line running through a pair of points and the reference line (the horizontal axis); as shown in Fig. 2a. For each direction, a log-log plot of variances against distances (for all $\mathbf{x}$ and $\Delta\mathbf{x}$ along the direction θ) is constructed and then, divided into overlapping subsets. A line is fitted to each subset and a set of Hurst coefficients are then calculated at individual scales using slopes of the subset lines fitted. The scale is the distance corresponding to the middle point of the subset (Fig. 2b).

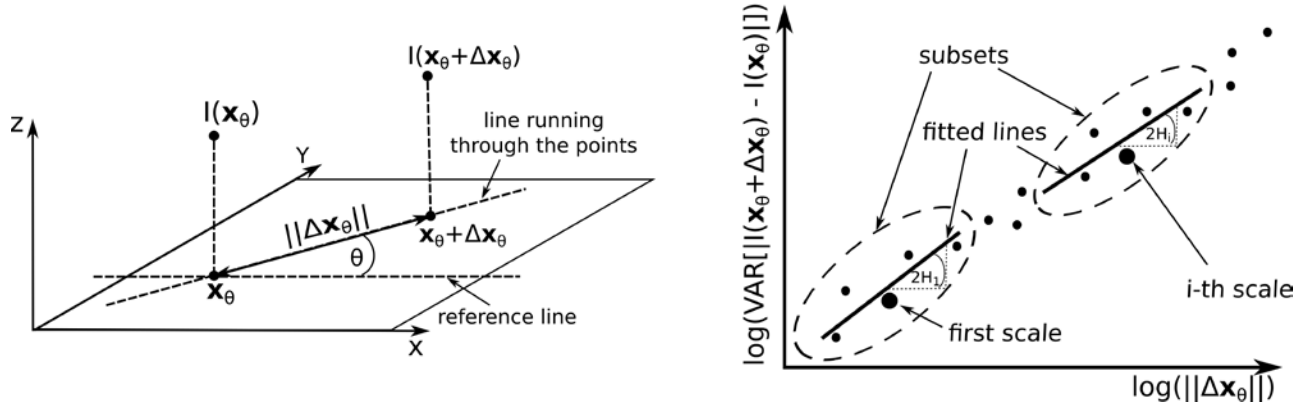

(a) (b)

Fig. 2. Schematic illustration of (a) the difference $\mathrm{I}(\mathbf{x}_\theta + \Delta\mathbf{x}_\theta) - \mathrm{I}(\mathbf{x}_\theta)$ and the distance $\|\Delta\mathbf{x}_\theta\|$ in direction θ and (b) the log-log plot of variances against distances for θ with the lines fitted to subsets and the Hurst coefficients. Scales are distances associated with the middle points of subsets.

5.2. Fractal parameters calculated using the VOT method

The Hurst coefficient is related to the fractal dimension (FD) as $\mathrm{FD} = 3 - \mathrm{H}$. At each scale a rose plot of the Hurst coefficients is constructed. An ellipse is fitted to the plot and the following two parameters are calculated (Fig. 3):

- Texture minor axis Sta. The parameter is defined as the half of minor axis length of the ellipse fitted. It represents dominating roughness component and relates to FD as FD_{Sta} = 3 - Sta.
- Texture aspect ratio Str. This parameter is the ratio of the minor axis and the major axis of the ellipse fitted. It measures surface anisotropy. For isotropic surfaces (i.e., surfaces exhibiting the same FDs in all directions), Str is equal to one. For anisotropic surfaces, Str is less than one.

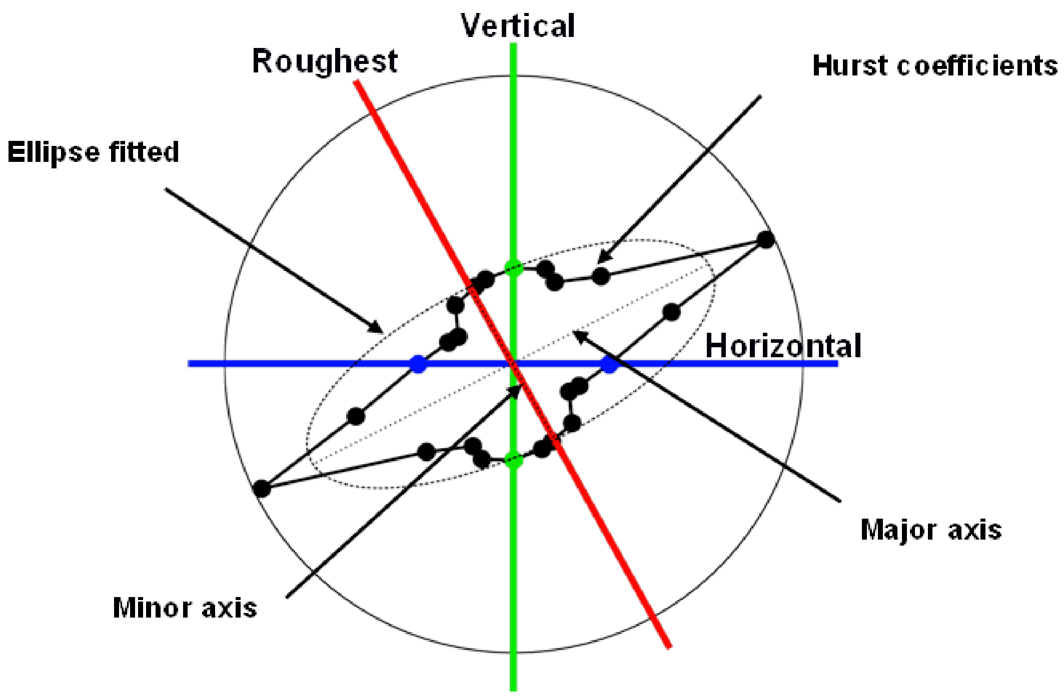

Fig. 3. A rose plot of Hurst coefficients with fitted ellipse and marked directions.

Mean (FD_{MEAN}), vertical (FD_V), horizontal (FD_H) and roughest (FD_{Sta}) fractal dimensions are the average values of FDs calculated at all individual scales and in all, vertical, horizontal and roughest directions respectively.

Sets of FD_V, FD_H, FD_{Sta}, Sta and Str calculated at individual scales are called the vertical, horizontal, roughest, texture minor axis and texture aspect ratio fractal signatures respectively.

5.3. Effects of acquisition conditions

The VOT method performs well in the presence of varying acquisition conditions, i.e., with noise up to 5%, magnification up to ×1.13, projection angle up to 10° and exposure variations up to 25 mAs [8].

The method is suitable for 8-bit images. The images have sufficient details for the evaluation of OA changes [9-12] and there were no statistically significant differences ($p \geq 0.065$, Student's t-test; unpublished data) between fractal parameters calculated for 8-bit and 16-bit images. For each bit-depth, 50 fractal texture surface images with the theoretical FD of 2.9 were generated. The high frequency FD was used to examine the effect of bit-depth with VOT results, since it contains high frequency components that are most affected by bit-depth.

6. Supplementary tables

Supplementary Table I. Baseline demographic characteristics of the subjects/knees divided by the radiographic incidence of knee OA cumulative to 84-month follow-up.

	Birmingham, AL (UAB) CR low resolution images			Iowa City, IA (UIowa) DF high resolution images		
Clinic site	ROA	No ROA	P value	ROA	No ROA	P value
Subject-based characteristics						
Total number of subjects	178	448		269	538	
Age, year, mean (SD)	61.3(7.3)	62.0(7.6)	0.3216	61.7(7.9)	61.4(7.7)	0.5339
Female, N (%)	131 (73.6)	249 (55.6)	<.0001	185 (68.8)	316 (58.7)	0.0056
White, N (%)	121 (68.0)	351 (78.3)	0.0066	260 (96.7)	530 (98.5)	0.083
BMI, kg/m^2, mean (SD)	30.5(5.4)	28.8(4.6)	0.0001	30.8(5.2)	29.0(4.8)	<0.001
Knee-based characteristics						
Total number of knees	195	699		303	855	
K-L grade, N (%):						
0	87 (44.6)	567 (81.1)	<0.001	155 (51.2)	721 (84.3)	<0.001
1	108 (55.4)	132 (18.9)		148 (48.8)	134 (15.7)	
Medial JSN grade, N (%):						
0	151 (77.4)	636 (91.0)	<0.001	225 (74.3)	806 (94.3)	<0.001
1	44 (22.6)	63 (9.0)		78 (25.7)	49 (5.7)	
Medial osteophyte grade, N (%):						
0	126 (64.6)	626 (89.6)	<0.001	217 (71.6)	769 (89.9)	<0.001
1	69 (35.4)	73 (10.4)		86 (28.4)	86 (10.1)	
Lateral JSN grade, N (%):						
0	183 (93.8)	695 (99.4)	<0.001	292 (96.4)	854 (99.9)	<0.001
1	12 (6.2)	4 (0.6)		11 (3.6)	1 (0.1)	
Lateral osteophyte grade, N (%):						
0	157 (80.5)	675 (96.6)	<0.001	266 (87.8)	829 (97.0)	<0.001
1	38 (19.5)	24 (3.4)		37 (12.2)	26 (3.0)	
Malalignment, N (%):						
Varus (<178°)	70 (35.9)	257 (36.8)	0.973	124 (40.9)	332 (38.8)	0.2504
Neutral (178°÷182°)	83 (42.6)	292 (41.8)		121 (39.9)	385 (45.0)	
Valgus (>182°)	42 (21.5)	150 (21.5)		58 (19.1)	138 (16.1)	
Time to event, N (%):						
30m	76 (39.0)	96 (13.7)	<0.001	100 (28.7)	113 (13.3)	<0.001
60m	80 (41.0)	104 (14.9)		140 (46.2)	67 (7.8)	
84m	39 (20.0)	499 (71.4)		63 (20.8)	675 (78.9)	

Supplementary Table II. Baseline demographic characteristics of the subjects/knees divided by the increase of medial TF JSN ≥ 0.5 grade (both PA and lateral views) cumulative to 84-month follow-up.

	Birmingham, AL (UAB) CR low resolution images			Iowa City, IA (UIowa) DF high resolution images		
Clinic site	JSN ≥ 0.5	No JSN change	P value	JSN ≥ 0.5	No JSN change	P value
Subject-based characteristics						
Total number of subjects	126	500		193	614	
Age, year, mean (SD)	61.8 (7.1)	61.8 (7.7)	0.962	62.5 (7.9)	61.2 (7.7)	0.038
Female, N (%)	81 (64.3)	299 (59.8)	0.357	111 (57.5)	390 (63.5)	0.134
White, N (%)	95 (75.4)	377 (75.4)	0.999	186 (96.4)	604 (98.4)	0.092
BMI, kg/m^2, mean (SD)	31.2 (5.5)	28.8 (4.6)	<0.001	30.5 (5.0)	29.3 (5.0)	0.005
Knee-based characteristics						
Total number of knees	137	757		213	945	
K-L grade, N (%):						
0	66 (48.2)	588 (77.7)	<0.001	115 (54.0)	761 (80.5)	<0.001
1	71 (51.8)	169 (22.3)		98 (46.0)	184 (19.5)	
Medial JSN grade, N (%):						
0	93 (67.9)	694 (91.7)	<0.001	157 (73.7)	874 (92.5)	<0.001
1	44 (32.1)	63 (8.3)		56 (26.3)	71 (7.5)	
Medial osteophyte grade, N (%):						
0	92 (67.2)	660 (87.2)	<0.001	153 (71.8)	833 (88.1)	<0.001
1	45 (32.8)	97 (12.8)		60 (28.2)	112 (11.9)	
Lateral JSN grade, N (%):						
0	137 (100)	741 (97.9)	0.086	212 (99.5)	934 (98.8)	0.366
1	0 (0.0)	16 (2.1)		1 (0.5)	11 (1.2)	
Lateral osteophyte grade, N (%):						
0	113 (82.5)	719 (95.0)	<.001	197 (92.5)	898 (95.0)	0.140
1	24 (17.5)	38 (5.0)		16 (7.5)	47 (5.0)	
Malalignment, N (%):						
Varus (<178°)	66 (48.2)	261 (34.5)	0.001	114 (53.5)	342 (36.2)	<0.001
Neutral (178°÷182°)	59 (43.1)	316 (41.7)		77 (36.2)	429 (45.4)	
Valgus (>182°)	12 (8.8)	180 (23.8)		22 (10.3)	174 (18.4)	
Time to event, N (%):						
30m	62 (45.3)	99 (13.1)	<0.001	92 (38.0)	109 (11.5)	<0.001
60m	52 (38.0)	113 (14.9)		78 (36.6)	75 (7.9)	
84m	23 (16.8)	545 (72.0)		43 (20.2)	761 (80.5)	

Supplementary Table III. Baseline demographic characteristics of the subjects/knees divided by the increase of lateral TF JSN ≥ 0.5 grade (both PA and lateral views) cumulative to 84-month follow-up.

	Birmingham, AL (UAB) CR low resolution images			Iowa City, IA (UIowa) DF high resolution images		
Clinic site	JSN ≥ 0.5	No JSN change	P value	JSN ≥ 0.5	No JSN change	P value
Subject-based characteristics						
Total number of subjects	57	569		80	727	
Age, year, mean (SD)	62.5 (7.9)	61.8 (7.5)	0.495	64.2 (8.1)	61.2 (7.7)	0.001
Female, N (%)	48 (84.2)	332 (58.3)	<0.001	66 (82.5)	435 (59.8)	<.001
White, N (%)	41 (71.9)	431 (75.7)	0.524	79 (98.8)	711 (97.8)	0.574
BMI, kg/m^2, mean (SD)	29.8 (6.2)	29.3 (4.7)	0.411	30.2 (5.6)	29.5 (5.0)	0.230
Knee-based characteristics						
Total number of knees	59	835		86	1072	
K-L grade, N (%):						
0	33 (55.9)	621 (74.4)	0.002	58 (67.4)	818 (76.3)	0.065
1	26 (44.1)	214 (25.6)		28 (32.6)	254 (23.7)	
Medial JSN grade, N (%):						
0	57 (96.6)	730 (87.4)	0.036	76 (88.4)	955 (89.1)	0.839
1	2 (3.4)	105 (12.6)		10 (11.6)	117 (10.9)	
Medial osteophyte grade, N (%):						
0	47 (79.7)	705 (84.4)	0.333	67 (77.9)	919 (85.7)	0.050
1	12 (20.3)	130 (15.6)		19 (22.1)	153 (14.3)	
Lateral JSN grade, N (%):						
0	46 (78.0)	832 (99.6)	<.001	78 (90.7)	1068 (99.6)	<.001
1	13 (22.0)	3 (0.4)		8 (9.3)	4 (0.4)	
Lateral osteophyte grade, N (%):						
0	50 (84.7)	782 (93.7)	0.009	76 (88.4)	1019 (95.1)	0.009
1	9 (15.3)	53 (6.3)		10 (11.6)	53 (4.9)	
Malalignment, N (%):						
Varus (<178°)	11 (18.6)	316 (37.8)	<0.001	13 (15.1)	443 (41.3)	<0.001
Neutral (178°÷182°)	23 (39.0)	352 (42.2)		42 (48.8)	464 (43.3)	
Valgus (>182°)	25 (42.4)	167 (20.0)		31 (36.0)	165 (15.4)	
Time to event, N (%):						
30m	25 (42.4)	105 (12.6)	<0.001	23 (26.7)	122 (11.4)	<0.001
60m	22 (37.3)	123 (14.7)		35 (40.7)	81 (7.6)	
84m	12 (20.3)	607 (72.7)		28 (32.6)	869 (81.1)	

References

1. Sharma L, Song J, Felson DT, Cahue S, Shamiyeh E, Dunlop DD. The role of knee alignment in disease progression and functional decline in knee osteoarthritis. JAMA 2001;286:188-95.

2. LaValley MP, McLaughlin S, Goggins J, Gale D, Nevitt MC, Felson DT. The lateral view radiograph for assessment of the tibiofemoral joint space in knee osteoarthritis: its reliability, sensitivity to change, and longitudinal validity. Arthritis Rheum 2005;52:3542–7.

3. Felson DT, Nevitt MC, Yang M, Clancy M, Niu J, Torner JC, et al. A New Approach Yields High Rates of Radiographic Progression in Knee Osteoarthritis. J Rheumatol 2008;35:2047-54.

4. Sled EA, Sheehy LM, Felson DT, Costiqan PA, Lam M, Cooke TD. Reliability of lower limb alignment measures using an established landmark-based method with a customized computer software program. Rheumatol Int 2011;31:71–7.

5. Podsiadlo P, Wolski M, Stachowiak GW. Automated selection of trabecular bone regions in knee radiographs. Med Phys 2008;35:1870–83.

6. Pentland A. Fractal-based description of natural scenes. IEEE Trans Pattern Anal Machine Intell 1984;6:661-74.

7. Veenland JF, Grashius JL, van der Meer F, Beckers AL, Gelsema ES. Estimation of fractal dimension in radiographs. Med Phys 1996;23:585-94.

8. Wolski M, Podsiadlo P, Stachowiak GW. Directional fractal signature analysis of trabecular bone: evaluation of different methods to detect early osteoarthritis in knee radiographs. Proc Inst Mech Eng H 2009;223:211–36.

9. Messent EA, Ward RJ, Tonkin CJ, Buckland-Wright C. Differences in trabecular structure between knees with and without osteoarthritis quantified by macro and standard radiography, respectively. Osteoarthritis Cartilage 2006;14:1302-5.

10. Wolski M, Stachowiak GW, Dempsey AR, Mills PM, Cicuttini FM, Wang Y, et al. Trabecular bone texture detected by plain radiography and variance orientation transform method is different between knees with and without cartilage defects. J Orthop Res 2011;29:1161-7.

11. Woloszynski T, Podsiadlo P, Stachowiak GW, Kurzynski M, Lohmander LS, Englund M. Prediction of progression of radiographic knee osteoarthritis using tibial trabecular bone texture. Arthritis Rheum 2012;64:688-95.

12. Kraus VB, Feng S, Wang S, White S, Ainslie M, Brett A, et al. Trabecular morphometry by fractal signature analysis is a novel marker of osteoarthritis progression. Arthritis Rheum 2009; 60:3711–22.